Computational Materials Science 119 (2016) 46–51

Contents lists available at ScienceDirect

Computational Materials Science

journal homepage: www.elsevier.com/locate/commatsci

Viscoelastic properties of randomly entangled carbon nanotube networks under cyclic tension loading

Chao Wang, Shaohua Chen *

LNM, Institute of Mechanics, Chinese Academy of Sciences, Beijing 100190, China

ARTICLE INFO

Article history:
Received 14 December 2015
Received in revised form 25 March 2016
Accepted 27 March 2016
Available online 12 April 2016

Keywords:
CNT networks
Viscoelasticity
Coarse-grained molecular dynamic simulation
Microstructure

ABSTRACT

As one of the promising nano-materials for energy absorption and dissipation, viscoelastic properties of randomly entangled carbon nanotube (CNT) networks subjected to cyclic tension loading are investigated with coarse-grained molecular dynamic simulations (CGMD). The effect of temperature, loading frequency, pre-strain of carbon nanotubes, physical binders and chemical crosslinks on the storage and loss moduli of CNT networks as well as the micro-mechanical mechanisms is mainly focused. Not only the storage modulus but also the loss one is found to be independent of the temperature. However, both of them can be enhanced greatly by the bundle-rich microstructures induced by pre-strain. Furthermore, physical binders and chemical crosslinks can also be used to tune the viscoelastic properties of CNT networks. All the findings should be helpful not only for understanding the mechanical mechanism of CNT networks but also for optimal designs of advanced energy absorption and dissipation materials.

1. Introduction

In recent ten years, carbon nanotubes (CNTs), as a new building block, have been used to assemble macroscopic materials, such as buckypapers [1], sponges [2], fibers of yarns [3], foams [4], aerogels [5,6] and composites [7]. In these novel materials, carbon nanotubes are randomly entangled with bundled microstructures to form complex networks, which exhibit series of advantages, including high specific surface areas, excellent thermostability, high thermal conductivity and low density [1–7]. Furthermore, CNT networks own special viscoelastic properties in contrast to the conventional materials besides a high storage modulus [8]. Xu et al. [1] synthesized CNT network materials with randomly long interconnected carbon nanotubes, which exhibit temperature-independent and frequency-independent viscoelastic properties. A similar frequency-independent viscoelastic property of CNT brushes/bundles has also been found in the nanoindentation test [9,10].

The specific microstructure and the stiffness/strength property of CNT networks have been well studied [11–17], while only a few investigations [11,17] are focused on their viscoelastic behaviors. Using large scale coarse-grained molecular dynamic simulations (CGMD), Li and Kröger [11] and Yang et al. [17] reproduced the temperature- and frequency-independent viscoelastic properties [1] and discussed the energy dissipation mechanism. Li and Kröger [11] believed that the zipping–unzipping behavior of contacting CNTs should be a key factor responsible for the viscoelastic property and the inter-tube entanglement effect would play an important role in the energy dissipation process. Yang et al. [17] attributed the energy dissipation behavior to the suddenly unstable attachment–detachment among CNTs. In accordance with experiment [1], the viscoelastic property of CNT networks was studied with cyclic shear loading by both Li and Kröger [11] and Yang et al. [17]. How about the viscoelastic property of CNT networks under cyclic tension loading? Would the temperature- and frequency-invariant dissipative features still exist? How would the microstructure of CNT networks influence the viscoelastic properties under cyclic tension loading. Systematic study on this issue is actually needed, which should be important for the optimal fabrication of CNT networks under different extreme conditions.

As an ideal technique, coarse-grained molecular dynamic simulation (CGMD) has been well developed, which could carry out approximate real experiments numerically. The related coarse-grained potentials for single-, double- or multi-walled carbon nanotubes have also been successfully given [13,17–20] and well used in recent years to study the relationship between the nano/micro-structures and the mechanical properties of carbon nanotube networks. For examples, with the method of CGMD, the folding, fracture and self-assembly behaviors of carbon

* Corresponding author.
E-mail address: chenshaohua72@hotmail.com (S. Chen).

http://dx.doi.org/10.1016/j.commatsci.2016.03.037
0927-0256/

nanotubes have been studied by Buehler [21] and Cranford et al. [19]; Li and Kröger [11] and Yang et al. [17] uncovered the underlying mechanism of temperature- and frequency-independent dissipative behaviors in CNT networks; Xie et al. [15] and Wang et al. [14,16,22] investigated the effect of carbon nanotube properties, physical and chemical crosslinks on the mechanical properties of buckypapers.

In this paper, CGMD is adopted with the aim of systematically studying the viscoelastic properties of carbon nanotube networks under cyclic tension loading. Many influencing factors, such as the interface energy between CNTs, the network microstructures, physical and chemical crosslinks as well as a pre-strain on the network structures will be considered. The result would be helpful not only for comprehensive understanding the mechanical behaviors of CNT networks but also for the future design of CNT networks with specified properties under extreme conditions.

2. Numerical model and methodology

2.1. Coarse-grained molecular dynamics

In view of the space–time restriction in full-atom MD simulations, a coarse-grained approach is adopted to characterize the mechanical behaviors of CNT networks [13,15], in which carbon nanotubes are discretized to a line of beads interacting through the internal bondings, angle springs and pair potentials, similar to a continuum model with a specified tensile stiffness, bending rigidity and an intertube binding energy. Within a single nanotube, the contribution of a stretching bond to the total energy is $E_T = k_T(r - r_0)^2/2$, where $k_T = YA/r_0$ is the spring constant with the Young's modulus Y, cross-section area A, the current distance r and the equilibrium one r_0. The contribution from a bead triplet bending is $E_B = k_B(1 + \cos\theta)$, where $k_B = 2D/r_0$ is the angular spring constant, D is the bending stiffness and θ the angle of the triplet. The interaction among beads in different CNTs abides by the van der Waals force, which ia described by the Lennard–Jones potential $E_{pair} = 4\varepsilon[(\sigma/r)^{12} - (\sigma/r)^6]$, with ε and σ denoting the depth of energy well and the distance at equilibrium, respectively. Similar to the existing literatures [14,22], the cutoff distance of the van der Waals interaction is chosen as 3 nm. The other parameters used in the present simulations are listed in Table 1, which were achieved by the calibration of full-atom MD simulations [13,19,21].

The physical (non-covalent) binder is modeled as a bead with a specified interface energy parameter $\gamma = 0.1\gamma_0 - 100\gamma_0$, where $\gamma_0 = 2.31 \times 10^{-10}$ J/m is the interface energy between CNTs [21]. The non-covalent binder represents some adhesive nanoparticles distributed randomly in CNT networks, such as carbon black, random polymer coils, graphene crumples or nanoplatelets.

The isothermal–isobaric (NPT) ensemble is used, and a Langevin thermostat 300 K and a Berendsen barostat 0 Pa are adopted in our simulations. The time-step is set to be 10 femtosecond. All the simulations are performed with the large-scale atomic/molecular massively parallel simulator (LAMMPS) [23].

Table 1
The force field parameters for a (5,5) carbon nanotube in the coarse-grained molecular dynamics [13,19,21].

Parameters	Values
Equilibrium interbead distance r_0 (Å)	10
Tensile stiffness parameter k (kcal mol^{-1} Å^{-2})	1000
Equilibrium angle α_0 (°)	180
Bending stiffness parameter k_B (kcal/mol)	14,300
Lennard–Jones parameter ε (kcal/mol)	15.1
Lennard–Jones parameter σ (Å)	9.35

2.2. Numerical samples

Fig. 1 shows the initial simulation box with a size of $120 \times 70 \times 3.4$ nm in three dimensions. Periodic boundary conditions are added in both the x and y directions, but a free one in the z direction. (5, 5) CNTs with a contour length of 100 nm are firstly constructed with an initial curvature reflecting the semiflexible feature and orientation fluctuation before being deposited layer by layer [13]. CNT networks are equilibrated by integrating Langevin equations of motion before the mechanical loading is applied. To accelerate the equilibrium process, a body force is initially applied downwards in the z direction with a rigid substrate below to generate a compact network, similar to the experimental procedure [1]. A Langevin thermostat is set as 300 K and a Berendsen barostat is set 0 Pa in x and y directions till the total energy fluctuation converges less than 0.1%. After that, both the force and the substrate are removed and a thin-film structure of CNT networks is maintained.

Due to a relatively large simulation scale, the distribution of intratube bond distances and angles is assumed to be approximately uniform in both the x and y directions. The thickness of the calculating system is defined as the maximum distance in the z direction. Several samples with different initial CNT densities are prepared. The thickness of CNT networks is found to increase as a linear function of the mass density initially and then converge to a constant at the density 0.28 g/cm^3, which is much close to the value reported for single-walled CNT buckypapers [24,25].

2.3. Dynamic mechanical analysis

The viscoelastic properties of networks are analyzed numerically by dynamic mechanical analysis (DMA), including the storage modulus, the loss one and the damping ratio. As a sinusoidal strain $\varepsilon = \varepsilon_0\sin(\omega t)$ is applied at one end of the network system in the x direction, a corresponding response of stress $\sigma = \sigma_0\sin(\omega t + \delta)$ will be activated as shown in Fig. 2, where ε_0 and σ_0 are the strain amplitude and the stress amplitude, respectively, δ is the phase angle, ω and t are the loading frequency and the loading time. The dynamic modulus is defined as $Y = Y' + Y''$, where $Y' = \sigma_0\cos\delta/\varepsilon_0$ and $Y'' = \sigma_0\sin\delta/\varepsilon_0$ are the tensile storage modulus and the loss one, respectively [11]. The damping ratio is denoted as $\tan\delta$. For the CNT buckypaper, it is not an isotropic material, but a porous one comprised of long CNT fibers, and its deformation is not homogeneous. The moduli under both cyclic tension and shear conditions are not constant as found in [11,26], but strain-dependent. Here, the amplitude of cyclic loading strain is set to be a smaller constant 0.015 to ensure a linearly viscoelastic deformation and eliminate the influence of strain amplitude.

In dynamic mechanical simulations, the condition of 0 Pa is maintained in y direction as the cyclic tensile loading is imposed in x direction.

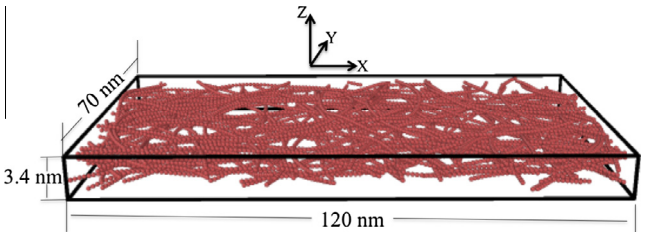

Fig. 1. The semi-two-dimensional coarse-grained molecular dynamics simulation model of a thin film formed by carbon nanotube networks subjected to a cyclic tension loading at the x-axis direction.

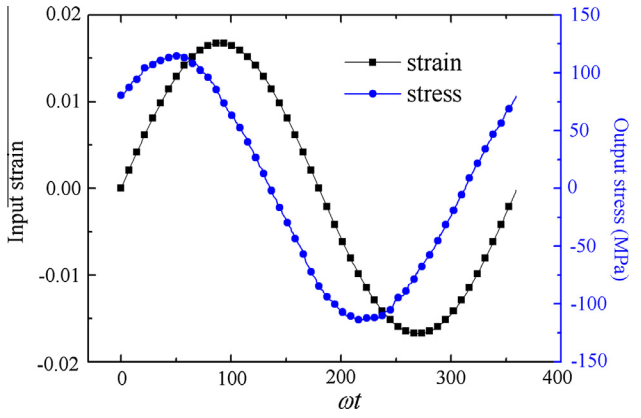

Fig. 2. The input cyclic tensile strain and the output cyclic tensile stress as a function of the phase degree for CNT networks at 300 K with a loading frequency of 2 GHz.

3. Results and discussion

3.1. Effect of temperature

A cycle tension loading is added on the network after the network is equilibrated at a given temperature. Fig. 3 shows the storage and loss moduli and the damping ratio as a function of the simulation temperature with a broad range from 100 to 1300 K. It is found that, though the CNT networks are subjected to cyclic tension loading, all three quantities are independent of the temperature, consistent well with the observations in existing experiments [1,26] and simulations [11,17] for CNT networks under cyclic shear loading, but significantly different from the traditional temperature-dependent polymer materials [8]. The temperature-independent viscoelastic feature of CNT networks may be ascribed to two main reasons. One is due to no big change in the microstructure when CNT networks stay in an enclosed space with different temperatures as shown in Fig. 3(b). The other is due to the temperature-insensitive van der Waals interaction among carbon nanotubes.

3.2. Effect of a pre-strain

Recent experiment finds that both the storage modulus and the loss one of CNT networks increase if the CNT network is stretched to 2% and 5% [26]. Inspired by the experiment finding [11] and a numerical result that the stiffness and strength of CNT networks can be tuned efficiently due to the network microstructures changed by a pre-strain [15], the viscoelastic property of CNT networks is further studied here with CGMD. The well-equilibrated networks after stretching with different pre-strains are shown in Fig. 4a–c. They are not be damaged after such a pre-stretching treatment. From our previous studies [14,16,22], if no chemical crosslink is introduced into the CNT networks, they will exhibit excellent ductility and could not be broken as the external tensile strain up to 1. Experimental work [1] also found that the CNT network materials will not be damaged under a shear strain up to 1000%. In the pre-stretching process, the microstructure in CNT networks evolves drastically with carbon nanotubes reorienting along the tension direction and clustering to large bundles. The bundles become thicker and thicker when the pre-strain increases. The viscoelastic property of networks subjected to pre-strains is shown in Fig. 4d, where the pre-strain can tune not only the storage and loss moduli but also the damping ratio effectively. The storage modulus and the loss modulus increase as high as 8 and 4 times, respectively, when the pre-strain increases from 0 to 0.74. Due to the formation of thick CNT bundles, the interface friction area increases, which leads to more energy consumption in the loading–unloading process. The elastic energy induced by the tension of carbon nanotubes also increases due to the enhanced interface strength, resulting in an increasing storage modulus. Therefore, the pre-strain technique should be an effective way to adjust the viscoelastic property of CNT networks.

3.3. Effect of the loading frequency

The effect of the tension frequency ω on the viscoelastic property of CNT networks is shown in Fig. 5 for a wide frequency range of 10–10^6 MHz, where the storage modulus increases very slowly in the region of low frequencies and then increase sharply in the region of high frequencies, while the loss modulus also increases very slowly in the region of low frequencies and then decreases after achieving a maximal value ~5 GPa at the frequency of about 10^4 MHz. At the relatively low frequency interval 10–10^3 MHz, both the storage modulus and the loss one can be regarded as a frequency-invariant region [11,17], in excellent agreement with the experiment observations [1], though the cyclic tension loading is adopted in the present simulations. The unstable attachment–detachment among CNTs or the zipping–unzipping of neighboring CNTs occur more quickly (on a timescale less than 1 ns and called

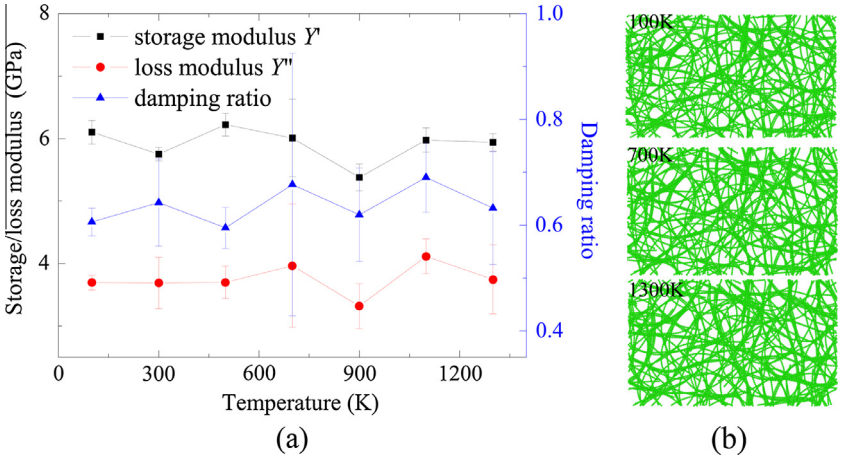

Fig. 3. The temperature effect on the viscoelasticity of CNT networks: (a) the storage and loss moduli and the damping ratio as a function of the temperature, where it shows the three parameters insensitive to the temperature; (b) similar microstructures of CNT networks at different temperatures.

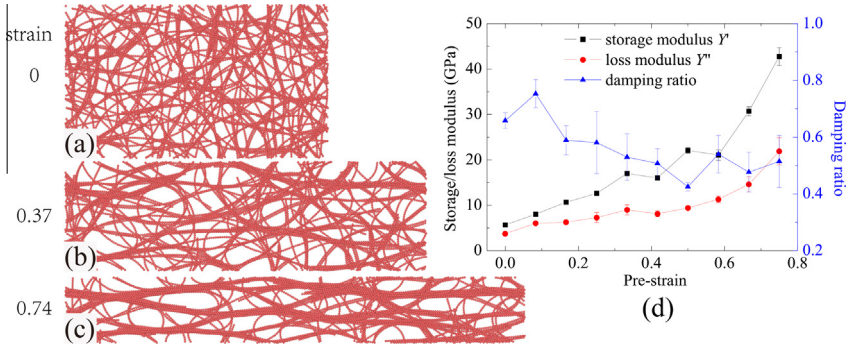

Fig. 4. The effect of pre-strain on the viscoelasticity of CNT networks: (a–c) the equilibrium microstructures of CNT networks under different pre-strains; (d) the storage and loss moduli and the damping ratio varying with the pre-strain.

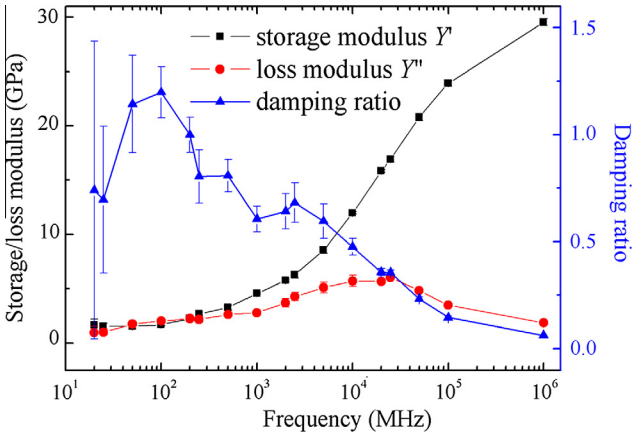

Fig. 5. The effect of the loading frequency on the viscoelasticity of CNT networks.

as an intrinsic frequency) than the applied loading so that the energy dissipation shows frequency-invariant [11,17]. However, the former works [11,17] did not study the case in higher frequency range 10^3–10^5 MHz, if the loading frequency is larger than the intrinsic one of CNT networks $\sim 10^3$ MHz, both the storage modulus and the loss one will be strong frequency-dependent as shown in Fig. 5. This aspect would be further checked by experiment in the future if possible.

3.4. Effect of physical binders

Due to the pore structure in CNT networks, some nanoparticles may be filled in as physical binders as shown in Fig. 6. Fig. 6a shows the initial state of a CNT network filled in nanoparticles with the volume fraction of 33.3%. After equilibrium relaxation, the discrete nanoparticles aggregate near the carbon nanotube junctions as shown in Fig. 6b for form small clusters. Under a cyclic tension loading, small clusters will further aggregate to form large ones accompanying with the reself assembly of CNT bundle structures. The final microstructure is given in Fig. 6c under a cycle tension loading with the maximum amplitude of strain 0.37. All the aggregation phenomena were actually found in real experiments [26,27] and numerical calculations [22]. How about the effect of physical binders on the viscoelastic property? Fig. 7 shows the storage modulus and the loss one as functions of the loading frequency for different volume fractions and interface energies of physical binders. As shown in Fig. 7a and b, the varying behavior of both the storage and loss moduli of CNT networks with physical binders of different volume fractions and interface energies via the loading frequency is similar to the case without physical binders shown in Fig. 5, in

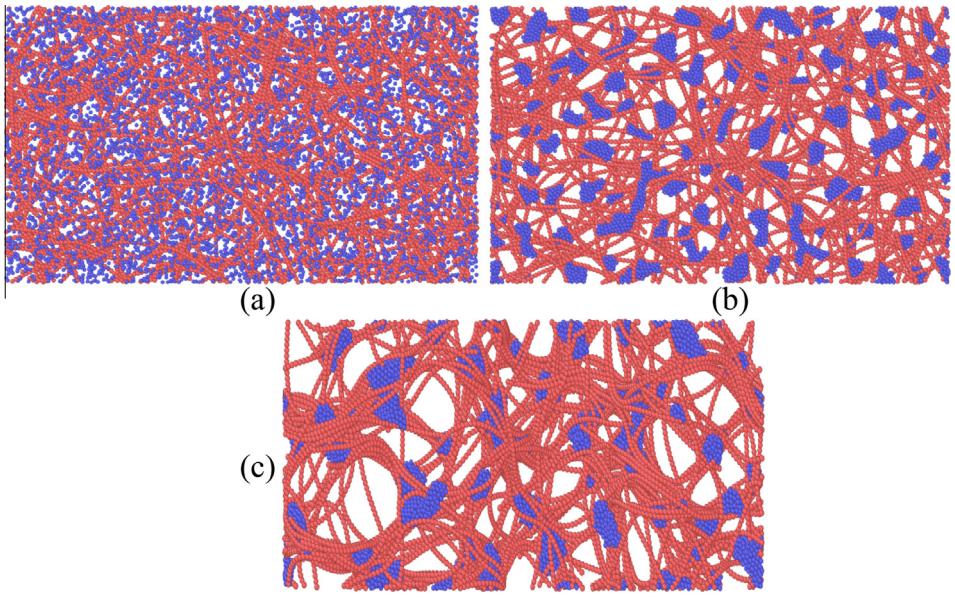

Fig. 6. Microstructures of CNT networks filled by physical binders: (a) the initial state; (b) after the structural relaxation; (c) after five loading cycles with the maximal strain 0.37.

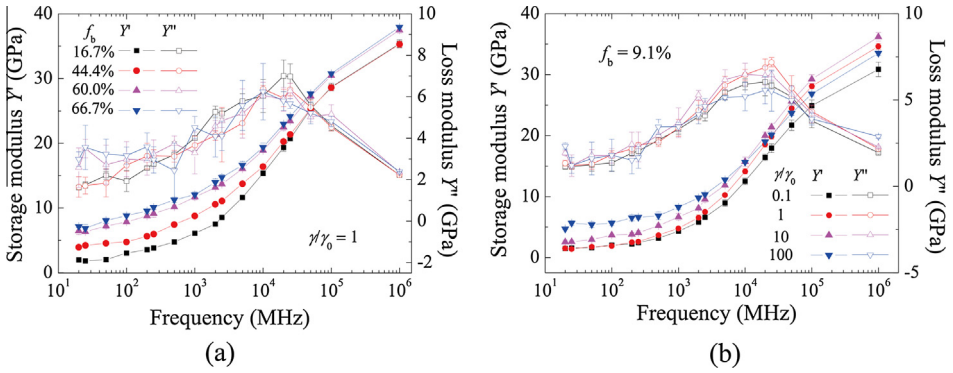

Fig. 7. The effect of physical binders on the viscoelasticity of CNT networks: (a) the storage and loss moduli varying with the loading frequency for different volume fractions of physical binders; (b) the storage and loss moduli varying with the loading frequency for different interface energies of physical binders.

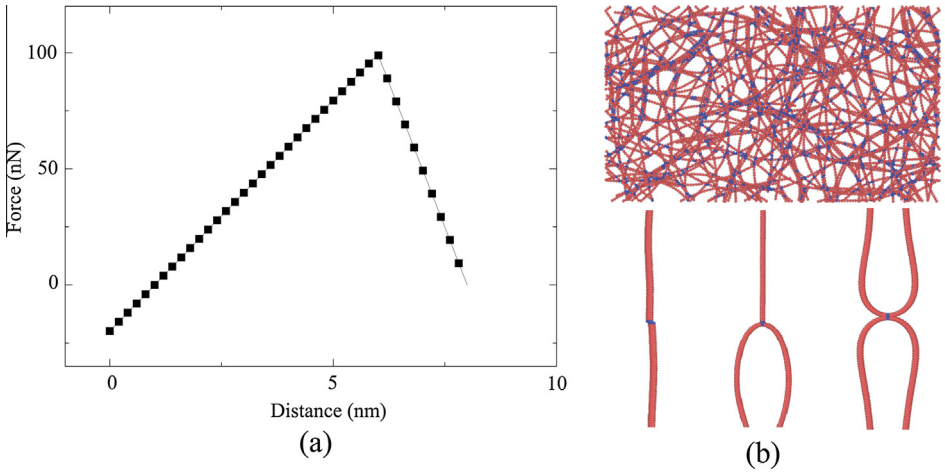

Fig. 8. The chemical crosslinks: (a) the force–length relation of a single crosslink; (b) the microstructure of CNT networks with chemical crosslinks (blue beads) at the joint among fibers (red color). (For interpretation of the references to colour in this figure legend, the reader is referred to the web version of this article.)

which the storage and loss moduli remain approximately frequency-invariant in the region of low loading frequencies and become frequency-sensitive in the region of high ones. Furthermore, the frequency-invariant storage modulus increases slightly with an increasing volume fraction or an increasing interface energy of physical binders, while the loss modulus does not sense the two factors. It further demonstrates that the experiment observation of frequency-invariant dissipative behavior of CNT networks is not resulted from the existence of physical binders, but the comparison of intrinsic frequency of microstructures and the external loading one.

3.5. Effect of chemical crosslinks

In experiments, chemical crosslinks could be formed by covalent bonds, coordination complex, cooperative hydrogen bonds, etc. Without loss of generality, we use a crosslink model here with a relaxed length of 1 nm. The tensile stiffness of the crosslink is 19.8 N/m and a peak force of 99.2 nN will be produced at a distance of $d = 6$ nm. The corresponding tensile force–distance relationship of a single crosslink is given in Fig. 8a. The interaction between CNTs connected by crosslinks is assumed to be pairwise, which vanishes for a large enough distance and recovers once the pair of crosslinking sites lies in the interaction range. Fig. 8b gives the microstructures of CNT networks with randomly distributed chemical crosslinks after equilibrium as well as three typical crosslinking subunits appearing in microstructures. When the density of crosslinks (highlighted by blue color) is 10.7 linkers per fiber, the viscoelastic properties of CNT networks is studied preliminarily as shown in Fig. 9. In comparison with the CNT networks without chemical crosslinks, both the storage modulus and the loss one of CNT networks are improved about two times by the chemical

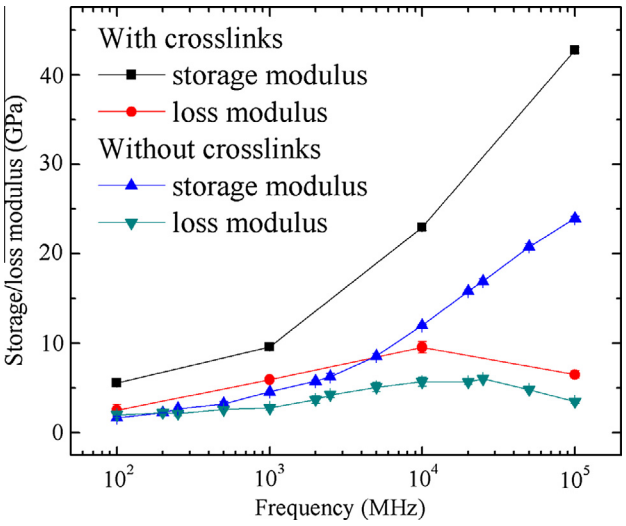

Fig. 9. The effect of chemical crosslinks on the storage and loss moduli of CNT networks, where the result without chemical crosslinks is given for comparison.

crosslinks. It is easy to infer that either the attachment/detachment behavior of CNTs or the zipping/unzipping one in microstructures would be influenced by the chemical crosslink between CNTs, leading to tunable viscoelastic properties of CNT networks.

4. Conclusions

A coarse-grained molecular dynamics model is adopted to investigate the viscoelasticity of carbon nanotube networks under cyclic tension loading. The effect of temperature, loading frequency, pre-strain, physical binders and chemical crosslinks on the storage and loss moduli as well as the damping ratio of CNT networks is considered. The temperature-independent viscoelastic property is found to be consistent well with the experiment observation [1,26]. However, the frequency-invariant property observed in experiment can be re-produced by CGMD only when the loading frequency is less than or near the intrinsic one of the network. Otherwise, the viscoelastic properties will be sensitive to the loading frequency. Both the storage modulus and the loss one can be improved by a pre-strain due to the induced bundle-rich microstructure, which agrees well with the experimental finding [26]. In addition, the effect of randomly distributed physical binders and chemical crosslinks on the viscoelastic properties is also discussed preliminarily. It is proved that the frequency-invariant dissipative behavior of CNT networks is not resulted from the physical binders, but the viscoelastic properties of CNT networks can be tuned by chemical crosslinks. These results would be helpful not only for understanding the mechanical mechanism of CNT networks but also for the design of CNT networks with novel properties.

Acknowledgement

The work reported here is supported by NSFC through Grants #11125211, #11372317, #11532013 and the 973 Nano-project (2012CB937500).

References

[1] M. Xu, D.N. Futaba, T. Yamada, M. Yumura, K. Hata, Science 330 (2010) 1364–1368.
[2] X. Gui, J. Wei, K. Wang, A. Cao, H. Zhu, Y. Jia, et al., Adv. Mater. 22 (5) (2010) 617–621.
[3] H.W. Zhu, C.L. Xu, D.H. Wu, B.Q. Wei, R. Vajtai, P.M. Ajayan, Science 296 (2002) 884–886.
[4] A. Cao, P.L. Dickrell, W.G. Sawyer, M.N. Ghasemi-Nejhad, P.M. Ajayan, Science 310 (2005) 1307–1310.
[5] M.B. Bryning, D.E. Milkie, M.F. Islam, L.a. Hough, J.M. Kikkawa, A.G. Yodh, Adv. Mater. 19 (5) (2007) 661–664.
[6] K.H. Kim, M. Vural, M.F. Islam, Adv. Mater. 23 (25) (2011) 2865–2869.
[7] F. Deng, M. Ito, T. Noguchi, L. Wang, H. Ueki, K. Niihara, et al., ACS Nano 5 (5) (2011) 3858–3866.
[8] R.S. Lakes, Viscoelastic Materials, Cambridge University Press, New York, 2009.
[9] S. Pathak, Z.G. Cambaz, S.R. Kalidindi, J.G. Swadener, Y. Gogotsi, Carbon 47 (2009) 1969–1976.
[10] S.B. Hutchens, L.J. Hall, J.R. Greer, Adv. Funct. Mater. 20 (14) (2010) 2338–2346.
[11] Y. Li, M. Kröger, Soft Matter 8 (30) (2012) 7822.
[12] Y. Li, M. Kröger, M. Kro, Carbon 50 (2012) 1793–1806.
[13] S.W. Cranford, M.J. Buehler, Nanotechnology 21 (26) (2010) 265706.
[14] C. Wang, B. Xie, Y. Liu, Z. Xu, ACS Macro Lett. 1 (10) (2012) 1176–1179.
[15] B. Xie, Y. Liu, Y. Ding, Q. Zheng, Z. Xu, Soft Matter 7 (21) (2011) 10039.
[16] C. Wang, E. Gao, L. Wang, Z. Xu, Comptes Rendus Mécanique 342 (5) (2014) 264–272.
[17] X. Yang, P. He, H. Gao, Nano Res. 4 (12) (2011) 1191–1198.
[18] J. Zhao, J.-W. Jiang, L. Wang, W. Guo, T. Rabczuk, J. Mech. Phys. Solids 71 (2014) 197–218.
[19] S. Cranford, H. Yao, C. Ortiz, M.J. Buehler, J. Mech. Phys. Solids 58 (2010) 409–427.
[20] X. Yang, P. He, H. Gao, Appl. Phys. Lett. 101 (5) (2012) 053105.
[21] M.J. Buehler, J. Mater. Res. 21 (11) (2006) 2855–2869.
[22] C. Wang, L. Wang, Z. Xu, Carbon 64 (2013) 237–244.
[23] S. Plimpton, J. Comput. Phys. 117 (1) (1995) 1–19.
[24] R.L.D. Whitby, T. Fukuda, T. Maekawa, S.L. James, S.V. Mikhalovsky, Carbon 46 (2008) 949–956.
[25] B. Ashrafi, J. Guan, V. Mirjalili, P. Hubert, B. Simard, A. Johnston, Compos. Part A Appl. Sci. Manuf. 41 (9) (2010) 1184–1191.
[26] Q. Liu, M. Li, Y. Gu, S. Wang, Y. Zhang, Q. Li, et al., Carbon 86 (2015) 46–53.
[27] K.H. Kim, Y. Oh, M.F. Islam, Nat. Nanotechnol. 7 (9) (2012) 562–566.